Physicochem. Probl. Miner. Process. 51(1), 2015, 83−94

www.minproc.pwr.wroc.pl/journal/

Physicochemical Problems of Mineral Processing

ISSN 1643-1049 (print)
ISSN 2084-4735 (online)

Received December 6, 2013; reviewed; accepted February 18, 2014

EFFECTS OF ACID LEACHING ON HALLOYSITE

Saruhan SAKLAR[*], Abdulkerim YORUKOGLU[**]

[*] General Directorate of Mineral Research and Exploration (MTA), Turkey, saklar@mta.gov.tr
[**] Department of Technology, Mineral Processing Division, Ankara, Turkey

Abstract: A characteristic iron-containing halloysite sample from Turkey was subjected to acid leaching using organic and inorganic acids for removing iron impurities. The aim of this study was to compare the raw hydrated and dehydrated halloysites with the leached products. Hydrochloric acid and oxalic acid were chosen as leaching agents for the removal of iron impurities at 80 °C for 2.5 h. The physicochemical properties of the acid-treated halloysite were analyzed by XRF, XRD, FTIR, TGA, DTA, SEM, and TEM. The XRF results showed that the acid treatment caused the dissolution of minor amounts of Al^{3+} ions from the clay layer. The XRD results indicated that the crystalline structure was unchanged after the leaching. However, it was observed that the hydrated (1 nm) halloysite readily lost its interlayer water and was transformed to the dehydrated (0.7 nm) form. In addition, no visible effects of the acid treatment on the tubular structure of halloysite were detected in the SEM and TEM images. Typical pores of varying dimensions were observed in all of the samples regardless of their form or treatment. Furthermore, the TG-DTA and FTIR analysis results were similar for both the raw and the acid-treated samples.

Keywords: *halloysite, kaolin, leaching, dehydration, characterization*

Introduction

Halloysite is a monoclinic clay mineral formed by surface weathering or hydrothermal alteration of alumina silicate minerals. It occurs in nature in two forms. The first form is called as hydrated halloysite, and its composition is $Al_2Si_2O_5(OH)_4 \cdot 2H_2O$ which can be easily identified by XRD (Murray, 2007). Hydrated halloysite readily and irreversibly loses its interlayer water even at ambient temperature and humidity (Churchman et al., 1984) to generate dehydrated halloysite ($Al_2Si_2O_5(OH)_4$). Attempts to differentiate this material from kaolin continue often by the application of intercalation methods (Joussein et al., 2007). A distinguishing property of halloysite is the inclusion of prismatic structures, mostly in the shape of cylindrical tubules, of sizes down to a few nanometers. Other shapes such as spheres and ellipsoids have also been reported depending on the geology of the deposit (Levis and Deasy, 2002). Hence, SEM is another important method for detecting the distinct prismatic halloysite

http://dx.doi.org/10.5277/ppmp150108

structures and differentiating dehydrated halloysite from kaolin, which is composed of plate-like structures.

As in kaolin ores, iron and titanium oxides and micas are the main discoloring impurities in halloysites. If the impurity content in clay concentrates is above the acceptable limits, product quality with respect to firing color, plasticity, and shrinkage declines. It is known from the literature that low quantities of fine iron oxides or hydroxides may cause strong pigmentation in kaolin (Pruett and Pickering, 2006). Therefore, it is typically necessary to remove or decrease the content of these impurities to the accepted *lowest standard level*, particularly if the material is to be used in ceramics. Although the beneficiation of halloysite is not a common issue, detailed studies have been carried out for kaolin (Ambikadevi and Lalithambika, 2000; Mandal and Banerjee, 2004; Arslan and Bayat, 2009). The leaching of iron oxides and the effect of their removal on the surface properties of kaolins have also been extensively studied (Mako et al., 2006; Panda et al., 2010).

Commercial halloysite deposits are located in northwestern Turkey, particularly in the Canakkale and Balikesir regions where mineralization occurred as a result of hydrothermal alterations (Ece and Schroeder, 2007). A large percentage of the deposits suffer from coloring due to the presence of fine iron oxide/hydroxide minerals such as hematite and goethite as well as minor quantities of muscovite, manganese, anatase, alunite, and even pyrite. The dark brownish-reddish-colored halloysites must be blended with white material or subjected to beneficiation by leaching in order to obtain saleable product.

In this study, a characteristic iron-containing halloysite sample from Turkey was subjected to acid leaching using organic and inorganic acids for removing the iron impurities. The raw hydrated and dehydrated halloysites were then compared with the leached products, and the variations in the physicochemical properties were analyzed by instrumental techniques such as SEM, XRF, XRD, FTIR, TG–DTA, and TEM.

Materials and methods

Iron-containing halloysite clay (2.50 g/cm^3) from one of the largest active mining zones (Balikesir-Gonen) in northwestern Turkey was selected for experimental studies. Raw massive hydrated (RMH) halloysite samples were collected for characterization. Raw powder hydrated (RPH) samples were then prepared stepwise using cone and roll crushers and a cup mill. Next, a representative amount of RPH (~500 g) was wet sieved at 90 μm, 30 μm, and 10 μm to determine the size distribution (Table 1).

Based on this analysis, it was determined that clay was dispersed, and that most of the particles were less than 10 μm in size. To provide homogeneity and simplicity, the fraction with the largest size (>90 μm) was neglected, and particles with sizes less

Table 1. Size distribution of the raw hydrated halloysite ore

Fraction (μm)	%Wt.
+90	3.03
−90 + 30	2.39
−30 + 10	3.17
−10	91.41

than 90 μm were chosen for the leaching tests by wet screening using a Russell screen (ϕ 52 cm). Before the wet screening, the clay sample was dispersed using a Denver 12 laboratory flotation machine without added dispersant at an agitation speed of 1500 rpm. The sieved slurry was then filtered, dried in a furnace above 70 °C, and powdered using a hand roller to provide the raw powder dehydrated sample (RPD).

XRD patterns were obtained with an X-ray diffractometer at 40 kV and 40 mA using Cu-Kα radiation and a step width of 0.08 (Bruker D8 Advance). SEM analyses (FEI Quanta 400 MK2) were performed on Au/Pd-plated samples, and for powder samples, a field emission gun (FEG) was used. The chemical compositions of the samples were determined using an XRF spectrometer (Philips Axios, *Almelo)*. FTIR spectra were recorded on a Thermo Scientific Nicolet 6700 (Madison, USA) spectrophotometer using KBr pellets. Thermogravimetric analyses were carried out using a Perkin Elmer *SII Exstar 6000 (*TG-DTA 6300) instrument. The sample was heated in a platinum crucible at a constant heating rate of 10 °C/min under a stream of dry air with a flow rate of 2 dm^3/min from 25 °C to 1000 °C. The tube morphologies were observed by transmission electron microscopy (TEM) analyses (FEI Tecnai G^2 F30). The samples were ultrasonically dispersed in ethanol, and then evaporated on a specimen holder before the TEM analysis.

Two types of leaching agents were chosen: oxalic acid ($(COOH)_2$) as the organic agent and hydrochloric acid (HCl) as the inorganic agent. The halloysite sample (15 g) was mixed with a 0.2–1.3 M solution of the acid (150 cm^3 at 80 °C for 2.5 h. To determine the effect of time on the leaching experiments, kinetic data were collected for 1.3 M HCl and 0.9 M $(COOH)_2$ solutions with a solid/liquid ratio of 10 at 80 °C from 15 to 150 min. Subsequently, the slurry was filtered, and the residue was washed with hot distilled water, dried, and analyzed by XRF.

Results and discussions

Leaching experiments

The results of the leaching experiments indicated that the dissolution of iron increased up to the acid concentrations of 0.25 M $(COOH)_2$ and 0.75 M HCl (Fig. 1a). Above

these concentrations, iron dissolution remained nearly constant, while at low acid concentrations, greater than 90% of Fe_2O_3 was removed.

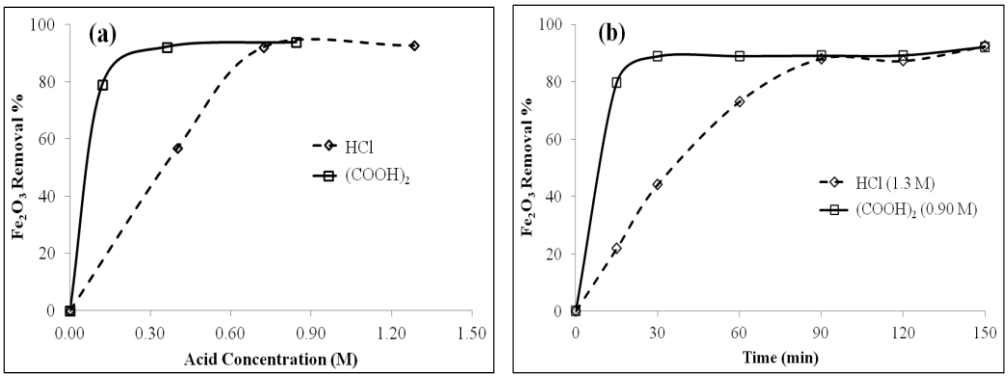

Fig. 1. Effect of acid concentration on (a) Fe_2O_3 removal and (b) reaction kinetics of raw halloysite

To compare the physicochemical properties of the raw and the acid-treated samples, the reactions with 1.30 M HCl and 0.90 M $(COOH)_2$ were investigated, and the products were evaluated. The highest concentration was selected for these studies to best observe the potential effects of the different acid treatments on the crystalline and tubular structures of halloysite.

The dissolution of Fe_2O_3 was observed to increase for up to 30 min and 90 min of the leaching time for the $(COOH)_2$ and HCl treatments, respectively (Fig. 1b) but then remained unchanged with a further increase in the leaching time. $(COOH)_2$ is a relatively fast leaching agent compared with HCl; even at a lower concentration, 90 % of iron was removed in 30 min using $(COOH)_2$, while this level was achieved only after 90 min of leaching with HCl at a higher concentration. The leaching potential of oxalic acid has already reported in several studies (Veglio et al., 1998; Ambikadevi and Lalithambika, 2000; Luevanos et al., 2011).

XRD characterization

First, the effect of the acid leaching on the structure of clay was investigated using XRD analysis (Fig. 2). The typical characteristic basal reflections (1 nm) of hydrated halloysite can be observed for the RMH and RPH samples. However, for the RPD, HCl, and $(COOH)_2$ samples, the broad 1nm peaks were displaced with 0.7 nm reflections, which are the equivalent basal reflections for dehydrated halloysite. The dehydration of the hydrated halloysite occurs because of the loss of the interlayer water, and consequently, the distance between the clay layers decreases from 1 nm to 0.7 nm (Churchman and Carr 1975).

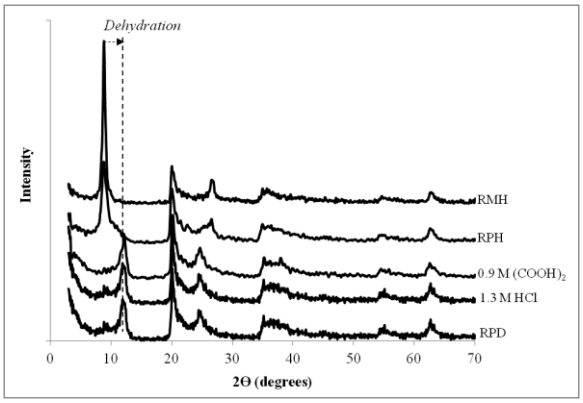

Fig. 2. XRD patterns of the raw and acid-treated halloysites

The XRD patterns of the acid-treated samples and raw halloysites were nearly the same except for the shift of the broad 1 nm peak of RMH. It has been reported that the reflection intensity of raw clay decreases and ultimately disappears (amorphous phase) as the acid treatment strength increases (Mako et al. 2006; Panda et al. 2010; Zhang et al. 2012). The current results (Fig. 1), however, suggest that the acid treatment under the conditions employed in this study did not affect the crystalline structure of halloysite. This lack of structural change must be attributed to the use of relatively low acid concentrations for leaching compared to those reported in the literature.

XRF characterization

The chemical analysis of the halloysite samples (Table 2) confirmed that the elemental composition of the raw samples was similar to the theoretical values for halloysite (Anthony et al., 1995) whether in the hydrated or dehydrated form. The difference between hydration and dehydration could not be observed by XRF due to the loss on ignition (LOI) that occurs during XRF analyses. The differences between the theoretical and measured values that were detected were due to the presence of the iron oxides/hydroxides such as goethite and hematite, and minor amounts of feldspar, anatase, alunite, muscovite, and/or illite (Saklar et al., 2012).

Table 2. Chemical analysis of the halloysite samples

Sample	SiO_2	Na_2O	MgO	Al_2O_3	P_2O_5	K_2O	CaO	TiO_2	Fe_2O_3	SO_3	LOI
Theoretical	46.54	-	-	39.50	-	-	-	-	-	-	13.96
RMH	44.10	<0.01	0.19	37.26	0.13	0.20	0.03	0.12	1.95	0.06	15.78
RPH	44.14	0.08	0.21	37.66	0.15	0.21	0.02	0.09	2.05	0.12	15.10
RPD	44.53	0.07	0.21	37.53	0.16	0.22	0.05	0.12	2.10	0.14	14.65
0.9M $COOH_2$	55.51	<0.01	0.19	29.22	0.02	0.24	0.03	0.14	0.16	0.03	14.35
1.3M HCl	48.63	<0.01	0.19	35.59	0.03	0.22	0.02	0.12	0.17	0.03	14.88

Furthermore, based on the XRF analyses, it was concluded that leaching of the halloysite sample with either acid led to an increase in the SiO_2 content and a decrease in the Al_2O_3 content. Thus, the Si/Al ratio also increased. A similar example of this behavior in halloysite treated with high acid concentrations was shown by Zhang et al. (2012), and it is thought to be due to the leaching of Al^{3+} ions from the clay layer via hydrolysis under acidic conditions. In addition, the content of K_2O, MgO, and TiO_2 remained practically unchanged, even at high acid concentrations. Therefore, the source of these compounds was attributed to muscovite and/or anatase, which cannot be directly removed by acid treatment alone (Yoon and Shi, 1986; Veglio et al., 1998; Oelkers et al., 2008).

TG/DTA analyses

Two weight-loss regions of nearly the same magnitude were detected in the TG/DTA analysis of the raw and acid-treated samples (Fig. 3). The DTA results verified that the TG curves resulted from water removal from the clay structure, which is a well-known phenomenon (Singer et al., 2004; Horvath et al., 2011). The first weight-loss region was below 90 °C and due to the loss of physisorbed or interlayer water. In parallel with the TG curves, the first endothermic peaks in the DTA analyses occurred at 40 °C for RMH and 5°C for RPH, both of which were hydrated samples, and indicated the loss of interlayer water at slightly lower temperatures. The dehydrated samples RPD, HCl, and $COOH_2$ exhibited initial endotherms between 60°C and 70°C due to the need for higher energy to achieve full dehydration (Joussein et al., 2006). The second distinctive weight loss occurred between 400°C and 550°C and resulted from the dehydroxylation of the clay sheet or the loss of structural water. This loss can be seen in the DTA curves as secondary broad endotherms between 485 °C and 495 °C that have very similar values. The successive exothermic peaks (between 990 and 995 °C) indicate the formation of the mullite phase in each sample (Sonuparlak et al., 1987).

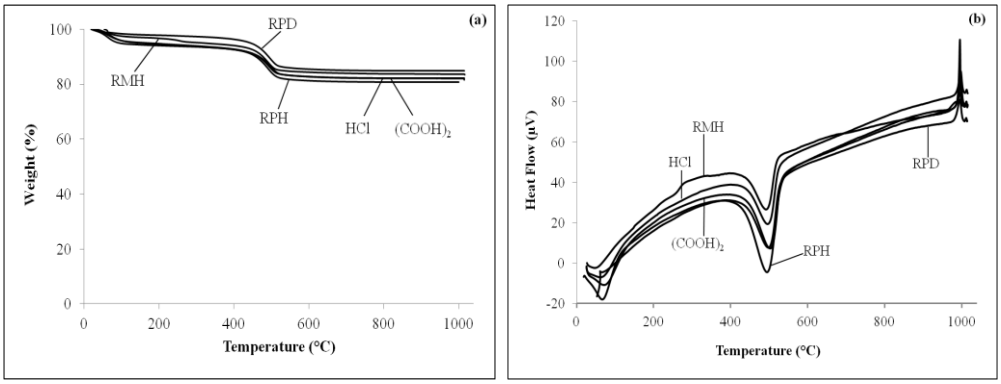

Fig. 3. a) TGA and b) DTA curves of the raw and acid-treated halloysites

The TG/DTA behavior of the raw halloysite samples was practically unchanged following the acid treatment under the conditions employed in this study. The small variations that can be noted are due to the conversion from the hydrated to the dehydrated form.

FTIR results

The IR spectrum of halloysite is characterized by an intense band at 459 cm^{-1} due to Si–O bending vibrations. The bands attributed to the Al–OH vibrations of the surface hydroxyl groups are observed at 744.5 and 792.7 cm^{-1} (Frost, 1995) or 746 and 796 cm^{-1} (Mellouk et al., 2009). The OH^- bending vibrations of the hydroxyl groups are observed at 910 cm^{-1} while the Si–O stretching region bands are observed at 1030 cm^{-1}, and the H–O–H (adsorbed water) deformation band appears at 1635 cm^{-1}. Finally, the characteristic OH^- stretching bands of halloysite can be observed at 3620, 3629, and 3696 cm^{-1} (Bobos et al., 2001; Frost et al., 2000).

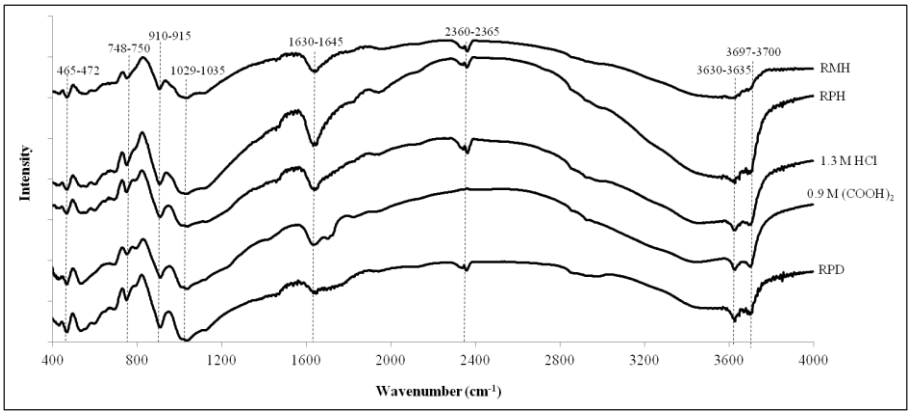

Fig. 4. FTIR spectra of the raw and acid-treated halloysites

In the FTIR spectra of the raw and the acid-treated samples (Fig. 4), the bands nearly match with only slight deviations. The bending bands for the Si–O (465–472 cm^{-1}), Al–OH (748–750 cm^{-1}), OH^- (910–915 cm^{-1}), and adsorbed water (1630–1645 cm^{-1}), and the stretching bands for Si–O (1029–1035 cm^{-1}) and OH^- (3630–3635 cm^{-1} and 3697–3700 cm^{-1}) are shifted to smaller values. The CO_2 bands (2360–2365 cm^{-1}) are also similar for each sample. This similarity of the FTIR spectra of the hydrated and the dehydrated raw samples may be ascribed to the relatively high degree of crystallinity. The similarity of the spectra for the raw and the acid-treated samples, nevertheless, proved that the acid concentrations used in this study were not sufficiently high to change the FTIR profiles.

SEM and TEM analyses

The SEM results (Fig. 5) for the halloysite sample indicated tubular particle morphology with most of the tubules having lengths of up to a few micrometers. No differences were observed in the morphology of the raw and the acid-treated samples, although the acid-treated samples were agglomerated (as if stacked together) when compared to the raw samples. This result may be attributed to the leaching, washing, and drying processes. It should be noted that SEM is a practical method for the analysis of bulk samples, but it is inappropriate for samples in powder form due to the difficulty of coating such samples. Not surprisingly, the micrographs of the bulk sample were therefore cleaner than those of the powders.

The TEM results (Fig. 6) give further information about the appearance and morphology of the particles in the halloysite samples. Typical hollow tubes with inner diameters as low as 10 nm were detected (Fig. 6). Again, no differences were observed for the raw and the acid-treated, or the hydrated and the dehydrated samples, respectively. Damage of the tubular structure has only been reported when the acid treatment was carried out at much higher concentrations (3 M H_2SO_4 at 90 °C for 8 hr (Zhang et al., 2012) and 5 N HCl at 70 °C for 4 hr (Belkassa et al., 2013).

Both smooth and porous surfaces were detected in the tubules, and the pores varied in size and shape independent of whether the samples were the raw or the acid-treated. Such pores in halloysites have been previously reported as a characteristic feature, and they have been shown to lead to particle size distribution and/or dehydration processes (Churchman et al., 1995). They may be generated during the analysis due to the transmission of electrons through the sample, which may cause the partial heating of the transmission zone.

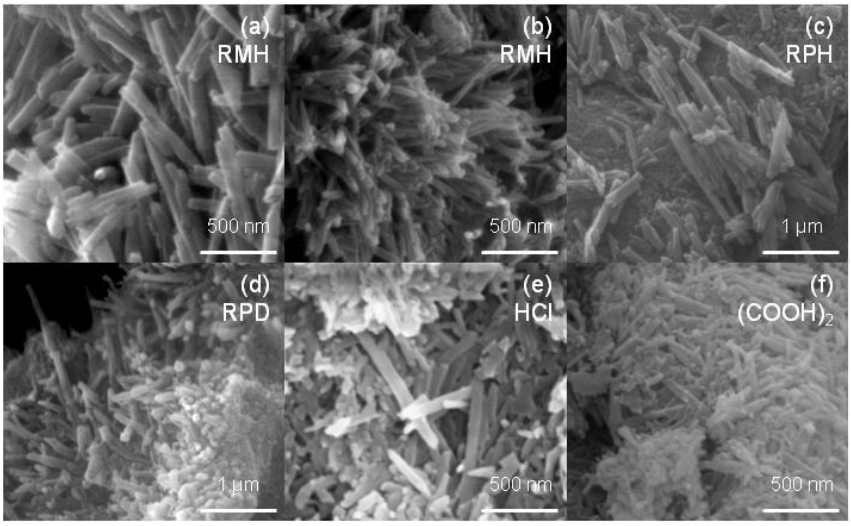

Fig. 5. SEM micrographs of the raw and acid-treated halloysites (a) and (b) raw massive hydrated (RMH) (c) raw powder hydrated (RPH) (d) raw powder dehydrated (e) HCl (f) $COOH_2$

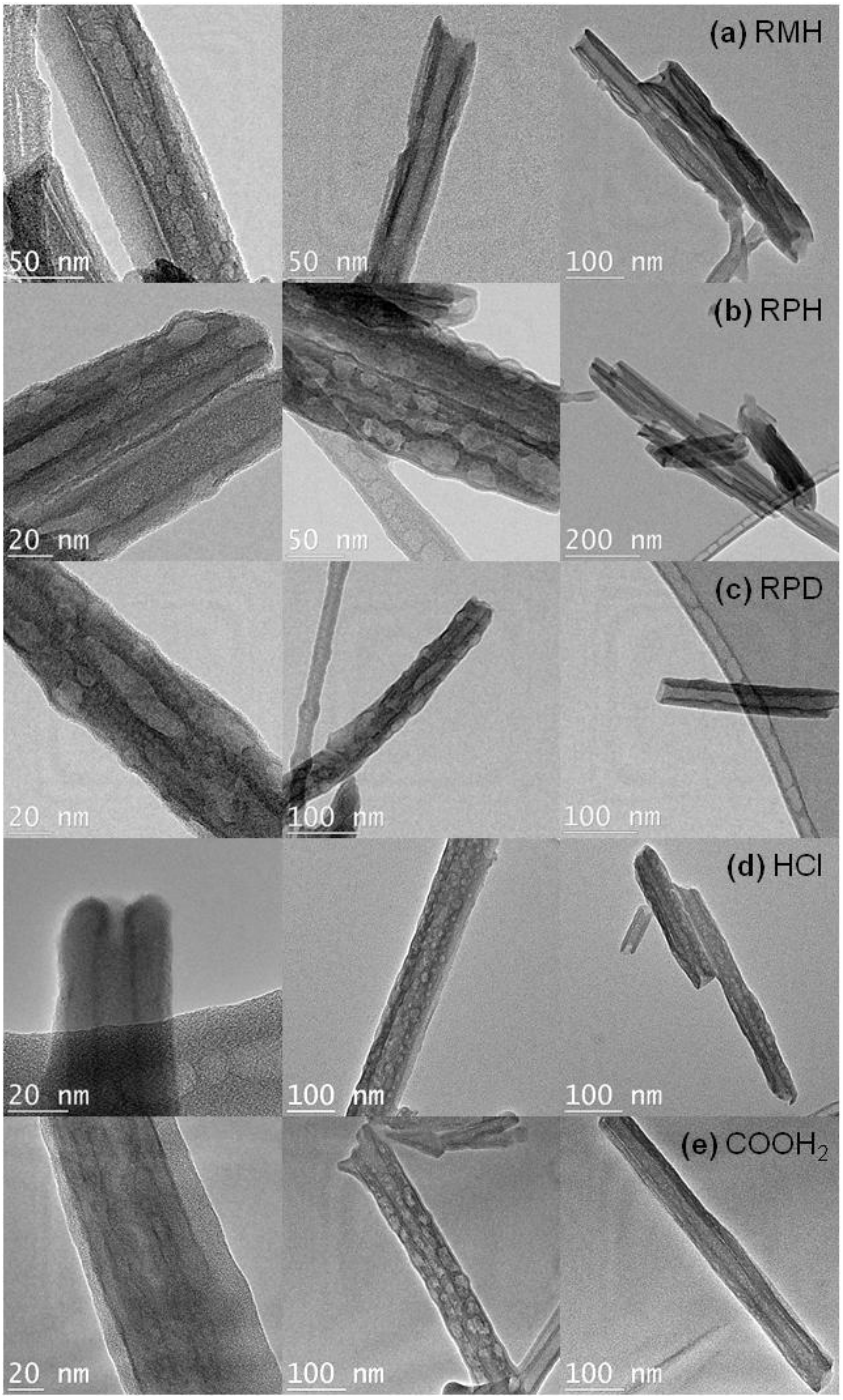

Fig. 6. TEM micrographs of the raw and acid-treated halloysites (a) raw massive hydrated (RMH) (b) raw powder hydrated (RPH) (c) raw powder dehydrated (d) HCl (e) $COOH_2$

Conclusions

Based on the results of this study, it was determined that iron can be removed from halloysite samples by chemical leaching without the deformation of the crystalline structure or changes in the particle morphology. Most of the iron (~90 %) in the samples tested was dissolved upon stirring with 0.25 M $(COOH)_2$ or 0.75 M HCl 10/1 liquid/solid ratio) for 2.5 hr at 80 °C.

The XRF results indicated that the SiO_2 content slightly increased while the Al_2O_3 content decreased with the acid treatment due to leaching of the Al^{3+} ions from the clay layer, which resulted in an increase in the Si/Al ratio. The XRD studies confirmed that hydrated (1 nm) halloysite readily lost interlayer water, and thus transformed into the dehydrated (0.7 nm) form, but without the deformation of the crystalline structure. Furthermore, no visible effect of the acid treatment on the particle morphology of halloysite was observed by the SEM and the TEM. From the SEM and TEM images, it was also determined that the halloysite particles are typically tubular in shape with diameters as low as 10 nm and lengths up to a few micrometers. Pores on the tubes were also detected in all of the samples independent of the acid treatment and the hydrated/dehydrated form. Finally, the TG-DTA and FTIR analysis results were also very similar for the raw and the acid-treated samples.

References

AMBIKADEVI V.R., LALITHAMBIKA M., 2000, *Effect of organic acids on ferric iron removal from iron-stained kaolinite*, Applied Clay Science, 16, 133-14.

ANTHONY J.W., BIDEAUX R.A., BLADH K.W., NICHOLS M.C., 1995, *Handbook of Mineralogy, Vol. II. Silica, Silicates, Mineral Data Publishing*, Tucson, Arizona.

ARSLAN V., BAYAT O., 2009, *Removal of Fe from kaolin by chemical leaching and bioleaching*, Clays and Clay Minerals, 57(6), 787–794.

BELKASSA K., BESSAHA F., MAROUF K., BATONNEAU I., COMPAROT J., KHELIFA A., 2013, *Physicochemical and adsorptive properties of a heat-treated and acid-leached Algerian halloysite*, *Colloids and Surfaces A: Physicochemical* and *Engineering Aspects*, 421, 26-33.

BOBOS I., DUPLAY J., ROCHA J., GOMES C., 2001, *Kaolinite to halloysite-7 A transformation in the kaolin deposit of Sao Vicente De Pereira-Portugal*, Clays and Clay Minerals, 49(6), 596-607.

CHURCHMAN G.J., CARR R.M., 1975, *The definition and nomenclature of halloysites*, Clays and Clay Minerals, 23, 382-388.

CHURCHMAN G.J., DAVY T.J., AYLMORE L.A.G., GILKES R.J., SELF P.G., 1995, *Characteristics of fine pores in some halloysites*, Clay Minerals, 30, 89–98.

CHURCHMAN G.J., WHITTON J.S., CLARIDGE G.G.C., THENG B.K.G., 1984, *Intercalation method using formamide for differentiating halloysite from kaolinite*. Clays and Clay Minerals, 32, 241–248.

ECE Ö.İ., SCHROEDER P.A., 2007, *Clay mineralogy and chemistry of halloysite and alunite deposits in the Turplu area-Balıkesir-Turkey*, Clays and Clay Minerals, 55(1), 18-35.

FROST R.L., 1995, *Fourier transform raman spectroscopy of kaolinite, dickite and halloysite*, Clays and Clay Minerals, 43(2), 191-195.

FROST R.L., KRISTOF J., HORVATH E., KLOPROGGE J.T., 2000, *Rehydration and phase changes of potassium acetate-intercalated halloysite at 298 K*, *Journal of Colloid* and *Interface Science*, 226, 318-327.

HORVATH E., KRISTOF J., KURDI R., MAKO E., KHUNOVA V., 2011, *Study of urea intercalation into halloysite by thermoanalytical and spectroscopic techniques*, Journal of Thermal Analysis and Calorimetry, 105, 53-59.

JOUSSEIN E., PETIT S., DELVAUX B., 2007, *Behavior of halloysite clay under formamide treatment*, Applied Clay Science, 35, 17–24.

JOUSSEIN E., PETIT S., FIALIPS C., VIEILLARD P., RIGHI D., 2006, *Differences in the dehydration-rehydration behavior of halloysites: new evidence and interpretations*, Clays and Clay Minerals, 54 (4), 473-484.

LEVIS S.R., DEASY P.B., 2002, *Characterization of halloysite for use as a microtubular drug delivery system*, *International Journal of Pharmaceutics*, 243, 125-134.

LUEVANOS A.M., DELGADO M.G.R., SALAS A.U., PEDROZA F.R.C., ALARCON J.G.O., 2011, *Leaching kinetics of iron from low grade kaolin by oxalic acid solutions*, Applied Clay Science, 51, 473–477.

MAKO E., SENKAR Z., KRISTOF J., VAGVÖLGYI V., 2006, *Surface modification of mechano-chemically activated kaolinites by selective leaching*, Journal of Colloid and Interface Science, 294, 362–370.

MANDAL S.K., BANERJEE P.C., 2004, *Iron leaching from China clay with oxalic acid: effect of different physico-chemical parameters*, International Journal of Mineral Processing, 74, 263–270.

MELLOUK S., CHERIFI S., SASSI M., MAROUF-KHELIFA K., BENGUEDDACH A., SCHOTT J., KHELIFA, A., 2009, *Intercalation of halloysite from Djebel Debagh (Algeria) and adsorption of copper ions*, Applied Clay Science, 44, 230–236.

MURRAY H.H., 2007, Applied Clay Mineralogy: Developments in Clay Science *2*, Elsevier, Amsterdam.

OELKERS E.H., SCHOTT J., GAUTHIER J.M., HERRERO-RONCAL T., 2008, *An experimental study of the dissolution mechanism and rates of muscovite*, Geochimica et Cosmochimica Acta, 72, 4948–4961.

PANDA A.K., MISHRAA B.G., MISHRAC D.K., SINGHA R.K., 2010, *Effect of sulphuric acid treatment on the physico-chemical characteristics of kaolin clay*, *Colloids and Surfaces A: Physicochemical* and *Engineering Aspects*, 363, 98-104.

PRUETT R.J., PICKERING S.M., 2006, *Kaolin*, Pp. 383-399 in: Industrial minerals and rocks: commodities, markets and uses (J.E. Kogel, N.C. Trivedi, J.M. Barker and S.T. Krukowski, editors) 7th edn. SME. Colorado,

SAKLAR S., AGRILI H., ZIMITOGLU O., BAŞARA B., KAAN U., 2012, *The characterization studies of the Northwest Anatolian halloysites/kaolinites*, Bulletin of the Mineral Research and Exploration, 145, 48-61.

SINGER A., ZAREI M., LANGE F.M., STAHR K., 2004, *Halloysite characteristics and formation in the northern Golan Heights*, Geoderma, 123, 279–295.

SONUPARLAK B., SARIKAYA M., AKSAY I.A., 1987, *Spinel phase formation during the 980°C exothermic reaction in the kaolinite-to-mullite reaction series*, Journal of the American Ceramic Society, 70 (11), 837-842.

VEGLIO F., PASSARIELLO B., BARBARO M., PLESCIA P., MARABINI A.M., 1998, *Drum leaching tests in iron removal from quartz using oxalic and sulphuric acids*, International Journal of Mineral Processing, 54, 183–200.

YOON R.H., SHI J., 1986, *Processing of kaolin clay*, Pp 366-379 in: Advances in Mineral Processing (P. Somasundran, Editor). AIME, New York.

ZHANG A., PAN L., ZHANG H., LIU S., YE Y., XIA M., CHEN X., 2012, *Effects of acid treatment on the physico-chemical and pore characteristics of halloysite, Colloids and Surfaces A: Physico-chemical* and *Engineering Aspects*, 396, 182–188.